Supplementary Information

Supplementary Table S1. Cell composition analysis across disease groups using Dirichlet aggression. Center, age, race and sex were included as covariates. Significance levels are indicated by asterisks (* FDR < 0.05, ** FDR < 0.01, *** FDR < 0.001).

celltype	coefficient	se	zval	pval	variable	FDR	significance
ECs	-0.2510	0.1840	-1.3640	0.173	diseaseLesional	0.2465	
ECs	-0.4588	0.1861	-2.4661	0.014	diseaseNon-lesional	0.0341	*
Eccrine.Cells	-0.0528	0.2911	-0.1813	0.856	diseaseLesional	0.8561	
Eccrine.Cells	-1.0029	0.2689	-3.7298	0.000	diseaseNon-lesional	0.0019	**
Fibroblasts	-0.2249	0.1484	-1.5154	0.130	diseaseLesional	0.2161	
Fibroblasts	-0.2389	0.1575	-1.5169	0.129	diseaseNon-lesional	0.1636	
Keratinocytes	0.1852	0.1761	1.0514	0.293	diseaseLesional	0.3625	
Keratinocytes	0.5533	0.1939	2.8531	0.004	diseaseNon-lesional	0.0144	*
LECs	-0.2386	0.1482	-1.6103	0.107	diseaseLesional	0.2161	
LECs	-0.4721	0.1509	-3.1284	0.002	diseaseNon-lesional	0.0088	**
Mast.Cells	-0.4017	0.1950	-2.0595	0.039	diseaseLesional	0.1315	
Mast.Cells	-0.3465	0.2135	-1.6228	0.105	diseaseNon-lesional	0.1636	
Myeloid.Cells	0.3650	0.1493	2.4448	0.014	diseaseLesional	0.0725	.
Myeloid.Cells	-0.2308	0.1411	-1.6354	0.102	diseaseNon-lesional	0.1636	
Pericytes	-0.2538	0.1620	-1.5670	0.117	diseaseLesional	0.2161	
Pericytes	-0.2686	0.1778	-1.5106	0.131	diseaseNon-lesional	0.1636	
Schwann.Melanocytes	0.1650	0.1681	0.9817	0.326	diseaseLesional	0.3625	
Schwann.Melanocytes	0.2345	0.1710	1.3713	0.170	diseaseNon-lesional	0.1892	
T.Cells	0.4386	0.1782	2.4611	0.014	diseaseLesional	0.0725	.
T.Cells	-0.1683	0.1789	-0.9408	0.347	diseaseNon-lesional	0.3468	
BKs	-0.1634	0.1704	-0.9589	0.338	diseaseLesional	0.4297	
BKs	0.2323	0.1642	1.4147	0.157	diseaseNon-lesional	0.3143	
CKs	0.8580	0.1420	6.0406	0.000	diseaseLesional	0.0000	***
CKs	0.2432	0.1256	1.9372	0.053	diseaseNon-lesional	0.1476	
DK1	-0.2564	0.1337	-1.9181	0.055	diseaseLesional	0.1438	
DK1	0.0940	0.1288	0.7296	0.466	diseaseNon-lesional	0.7243	
DK2	0.2636	0.1728	1.5255	0.127	diseaseLesional	0.2225	
DK2	-0.0607	0.1727	-0.3517	0.725	diseaseNon-lesional	0.8866	
DK3	-0.1011	0.1270	-0.7965	0.426	diseaseLesional	0.4806	
DK3	0.2407	0.1163	2.0698	0.038	diseaseNon-lesional	0.1347	
DK4	0.1323	0.1737	0.7617	0.446	diseaseLesional	0.4806	
DK4	0.0480	0.2148	0.2234	0.823	diseaseNon-lesional	0.8866	
DK5	0.1447	0.1257	1.1511	0.250	diseaseLesional	0.3659	
DK5	-0.1157	0.1193	-0.9705	0.332	diseaseNon-lesional	0.5806	
DK6	0.7716	0.1877	4.1107	0.000	diseaseLesional	0.0003	***
DK6	0.0097	0.1774	0.0548	0.956	diseaseNon-lesional	0.9563	
DK7	0.0338	0.2074	0.1628	0.871	diseaseLesional	0.8707	
DK7	-0.0501	0.1767	-0.2833	0.777	diseaseNon-lesional	0.8866	
FCs	0.2352	0.2094	1.1233	0.261	diseaseLesional	0.3659	
FCs	-0.0837	0.2020	-0.4143	0.679	diseaseNon-lesional	0.8866	
KK1	0.3315	0.2071	1.6003	0.110	diseaseLesional	0.2190	
KK1	-0.3208	0.1976	-1.6233	0.105	diseaseNon-lesional	0.2439	
KK2	-0.5440	0.2911	-1.8690	0.062	diseaseLesional	0.1438	
KK2	-0.9525	0.2909	-3.2739	0.001	diseaseNon-lesional	0.0050	**
SBs	-1.2356	0.3467	-3.5643	0.000	diseaseLesional	0.0017	**
SBs	-1.5141	0.3575	-4.2346	0.000	diseaseNon-lesional	0.0003	***
ECRs	-0.8134	0.3205	-2.5384	0.011	diseaseLesional	0.0390	*
ECRs	-1.2252	0.3310	-3.7009	0.000	diseaseNon-lesional	0.0015	**

Supplementary Table S2. Number and proportion of cells classified by fate probability thresholds toward KK1 or KK2 terminal states, including cells with fate probability > 0.7 toward KK2 (fasteProb_KK2_g0.7) and < 0.1 toward KK1 (fateProb_KK1_2_l0.1).

disease	group	total	prop_fateProb_KK2_g0.7	prop_fateProb_KK1_2_l0.1	prop_fateProb_KK1_2l0.1_KK2_g0.7	cell.num_fateProb_KK2_g0.7	cell.num_fateProb_KK1_2_l0.1	cell.num_fateProb_KK1_2l0.1_KK2_g0.7	prop_ovlp_KK1_2l0.1_KK2_g0.7
Healthy	ECRs	739	NA	0.79	NA	NA	584.00	NA	NA
Healthy	SBs	1414	NA	0.44	NA	NA	621.00	NA	NA
Healthy	DK4	7781	NA	0.00	NA	NA	10.00	NA	NA
Healthy	FCs	2311	NA	0.00	NA	NA	2.00	NA	NA
Healthy	DK7	2019	NA	0.00	NA	NA	1.00	NA	NA
Healthy	DK5	3108	NA	0.00	NA	NA	1.00	NA	NA
Healthy	DK2	10453	NA	0.00	NA	NA	3.00	NA	NA
Lesional	DK7	14069	0.66	0.65	0.65	9339.00	9181.00	9180.00	1.00
Lesional	KK1	20837	0.46	0.43	0.43	9508.00	9038.00	8978.00	0.99
Lesional	DK2	39451	0.23	0.22	0.22	8950.00	8860.00	8772.00	0.99
Lesional	KK2	2109	0.21	0.20	0.20	438.00	427.00	427.00	1.00
Lesional	DK4	23949	0.13	0.13	0.13	3232.00	3071.00	3025.00	0.99
Lesional	ECRs	1605	0.11	0.87	0.11	179.00	1403.00	174.00	0.97
Lesional	SBs	2653	0.10	0.75	0.10	264.00	1996.00	259.00	0.98
Lesional	FCs	10769	0.07	0.07	0.07	760.00	732.00	731.00	1.00
Lesional	DK5	8685	0.06	0.05	0.05	524.00	425.00	424.00	1.00
Lesional	CKs	7271	0.03	0.03	0.03	249.00	230.00	229.00	1.00
Lesional	DK1	36274	0.03	0.02	0.02	966.00	843.00	842.00	1.00
Lesional	DK6	2050	0.01	0.01	0.01	24.00	19.00	19.00	1.00
Lesional	DK3	23202	0.01	0.01	0.01	170.00	152.00	152.00	1.00
Lesional	BKs	23028	0.00	0.00	0.00	7.00	4.00	4.00	1.00
Non-lesional	DK2	16356	0.00	0.00	0.00	11.00	4.00	4.00	1.00
Non-lesional	KK1	3973	0.00	NA	NA	2.00	NA	NA	NA
Non-lesional	DK4	7452	0.00	0.00	NA	3.00	26.00	NA	NA
Non-lesional	FCs	4433	0.00	NA	NA	1.00	NA	NA	NA
Non-lesional	ECRs	524	NA	0.90	NA	NA	470.00	NA	NA
Non-lesional	SBs	658	NA	0.88	NA	NA	577.00	NA	NA

Supplementary Table S3. Endoplasmic reticulum (ER) and mitochondrial function-related pathways dysregulated in TWEAK-stimulated keratinocytes from a public bulk RNA-seq dataset (GSE171170).

source	term_name	term_id	comp	padj	dirt
GO:CC	endoplasmic reticulum lumen	GO:0005788	TWposIL_17_v_C	1.57E-07	up
GO:MF	oxidoreductase activity, acting on the aldehyde or oxo group of donors	GO:0016903	TWposIL_17_v_TWposTNF	0.00041413	up
GO:CC	endoplasmic reticulum lumen	GO:0005788	TWposTNF_v_C	1.10E-07	up
GO:CC	lumenal side of endoplasmic reticulum membrane	GO:0098553	TWposTNF_v_C	0.00022996	up
GO:MF	oxidoreductase activity, acting on the aldehyde or oxo group of donors	GO:0016903	TWposTNF_v_C	0.00406085	down
GO:BP	nitric oxide metabolic process	GO:0046209	TWposTNF_v_C	0.00445287	up
GO:BP	regulation of nitric oxide metabolic process	GO:0080164	TWposTNF_v_C	0.01406677	up
GO:MF	oxidoreductase activity, acting on CH-OH group of donors	GO:0016614	TWposTNF_v_C	0.03658205	down
GO:BP	cellular response to oxidative stress	GO:0034599	TWposTNF_v_C	0.04693609	up
GO:BP	response to oxidative stress	GO:0006979	TWposTNF_v_C	0.04836005	up
GO:CC	lumenal side of endoplasmic reticulum membrane	GO:0098553	TWposTNF_v_IL_17	0.00010223	up
GO:MF	oxidoreductase activity, acting on CH-OH group of donors	GO:0016614	TWposTNF_v_IL_17	0.00380544	down
GO:MF	oxidoreductase activity, acting on the aldehyde or oxo group of donors	GO:0016903	TWposTNF_v_IL_17	0.00503362	down
GO:MF	oxidoreductase activity, acting on the CH-OH group of donors, NAD or NADP as acceptor	GO:0016616	TWposTNF_v_IL_17	0.01113368	down
GO:BP	cellular response to oxidative stress	GO:0034599	TWposTNF_v_IL_17	0.04221359	up
GO:CC	endoplasmic reticulum lumen	GO:0005788	TWposTNF_v_TNF	0.01091029	up
GO:BP	nitric oxide metabolic process	GO:0046209	TWposTNF_v_TW	0.00140557	up
GO:CC	lumenal side of endoplasmic reticulum membrane	GO:0098553	TWposTNF_v_TW	0.00803863	up
GO:MF	oxidoreductase activity, acting on the aldehyde or oxo group of donors	GO:0016903	TWposTNF_v_TW	0.00944713	down
GO:BP	regulation of nitric oxide metabolic process	GO:0080164	TWposTNF_v_TW	0.01641866	up
GO:BP	positive regulation of nitric oxide metabolic process	GO:1904407	TWposTNF_v_TW	0.02057789	up
GO:BP	nitric oxide biosynthetic process	GO:0006809	TWposTNF_v_TW	0.02222927	up

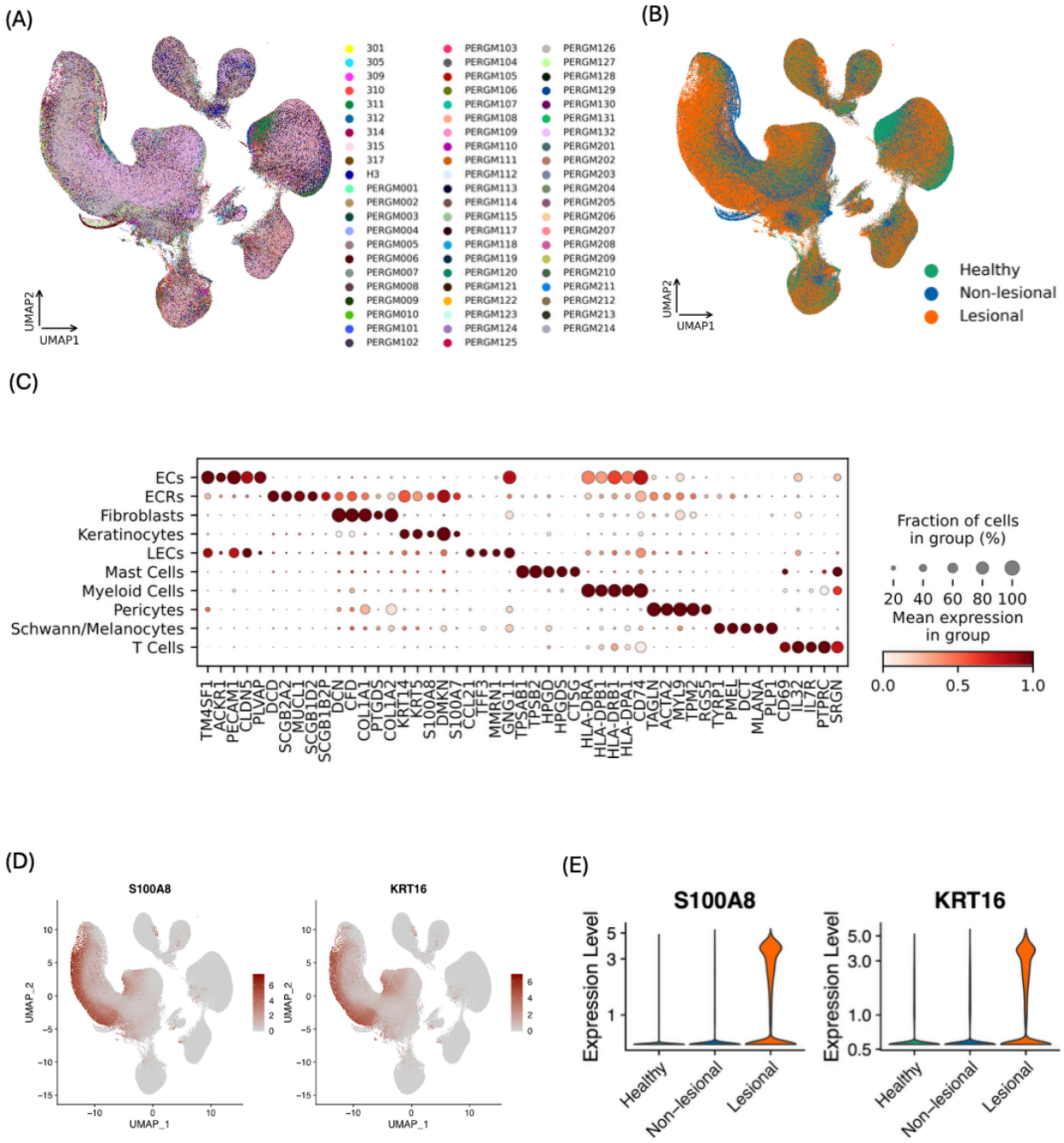

Supplementary Figure S1. Global cell population and characteristics. (A) UMAP colored by individual patients. (B) UMAP colored by tissue types. (C) Expression of the top five marker genes for individual cell types. (D) Feature plots showing expression of two inflammation-related genes, *S100A8* and *KRT16*. (E) Violin plots of *S100A8* and *KRT16* expression stratified by tissue types.

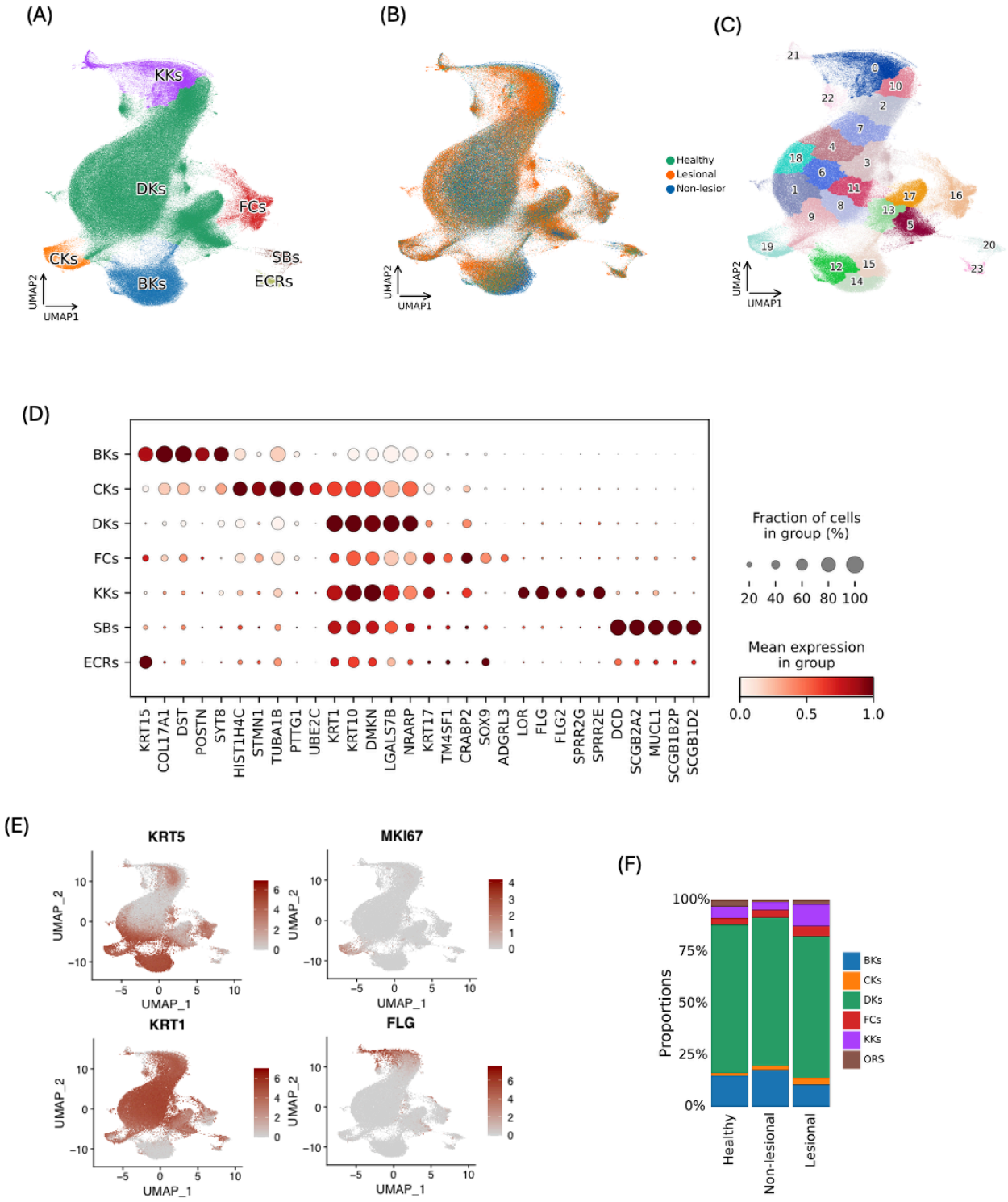

Supplementary Figure S2. Sub-clustering of keratinocytes. (A) UMAP colored by six major cell types of keratinocytes. (B) UMAP colored by tissue types. (C) UMAP colored by sub-clusters. (D) Expression of the top five marker genes for individual keratinocyte types. (E) Feature plots showing expression of four representative keratinocyte marker genes. (F) Proportions of keratinocyte cell types across individual tissue types.

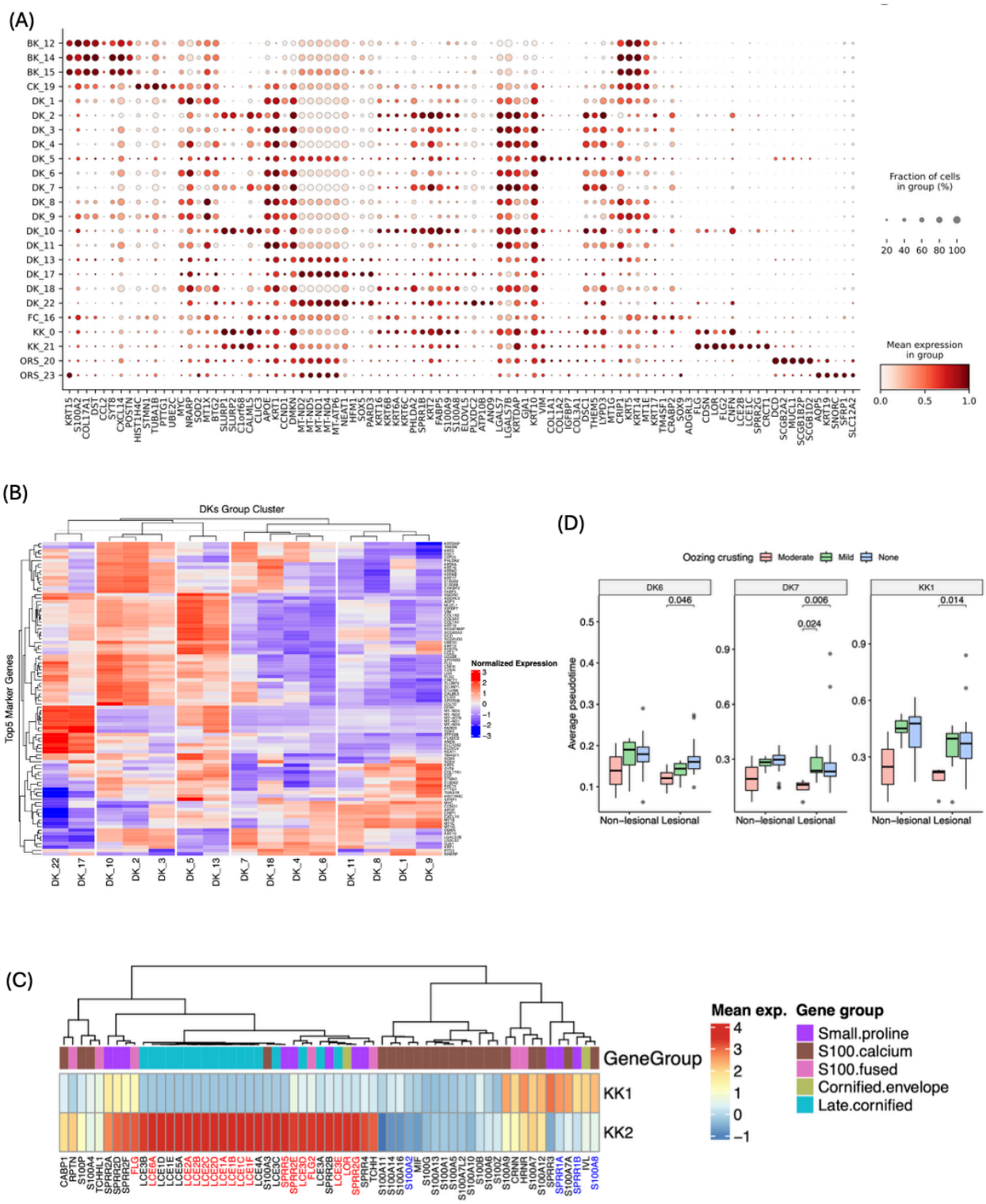

Supplementary Figure S3. Fine-grained keratinocyte subclusters. (A) Expression of the top five marker genes for each keratinocyte subcluster. (B) Heatmap showing hierarchical clustering of differentiated keratinocytes (DKs) subclusters based on expression of the top five marker genes. (C) Heatmap of average expression of Epidermal Differentiation Complex (EDC) genes in KK1 and KK2 subclusters. (D) Box plot showing average pseudotime of non-lesional (N = 37) and

lesional (N = 39) AD samples stratified by oozing and crusting severity (moderate, mild, or none), for DK6, DK7 and KK1 subclusters. Box plots display median (center line), interquartile range (box; 25th–75th percentiles), and whiskers extending to 1.5× IQR; outliers are shown as points beyond whiskers, and whisker limits define minimum and maximum values. Two-tailed Wilcoxon rank-sum test BH-adjusted $p < 0.05$ are shown.

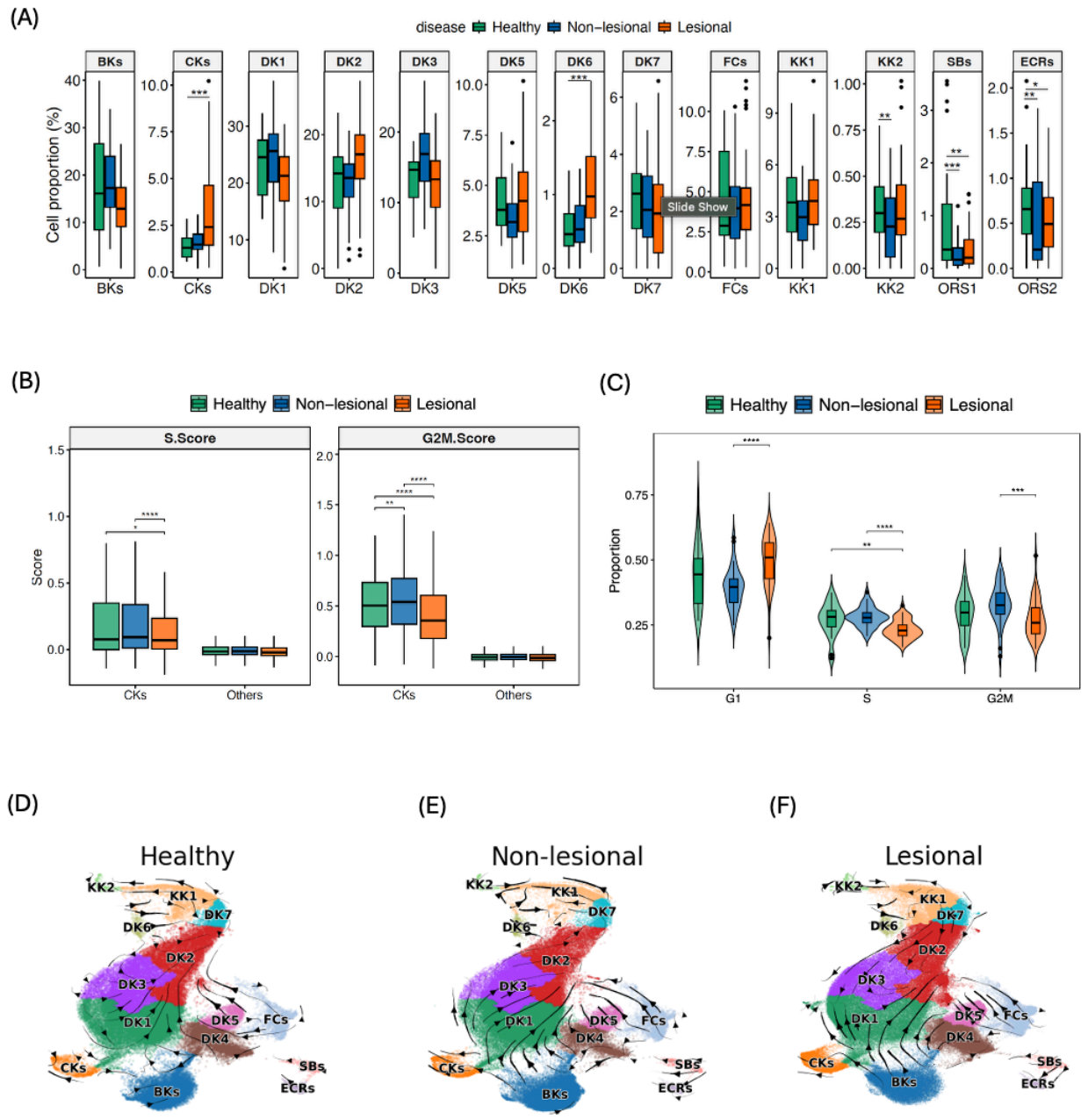

Supplementary Figure S4. Characteristics of the fine-grained keratinocyte subclusters. (A) Box plots showing cell proportions in individual subclusters, stratified by tissue types. Dirichlet regression (two-sided Wald test BH-adjusted $p < 0.05$ are shown (* p.adj < 0.05, ** p.adj < 0.01, *** p.adj < 0.001, **** p.adj < 0.0001). (B) Box plots of S and G2M scores in cycling keratinocytes (CKs) compared to other keratinocyte types**.** (C) Violin plots showing the distribution of cycling state (G1, S and G2M) in individual tissue types. (B-C) Two-sided Wilcoxon rank-sum test BH-adjusted p values < 0.05 are shown (* p.adj < 0.05, ** p.adj < 0.01, *** p.adj < 0.001, **** p.adj < 0.0001). (D-F) RNA velocity stream plots for healthy, non-lesional and lesional AD samples, separately. Box plots display median (center line), interquartile range

(box; 25th–75th percentiles), and whiskers extending to 1.5× IQR, with whisker limits defining the minimum and maximum values within this range. A total of 23 healthy, 39 non-lesional and 54 lesional samples were included in plots (A-C).

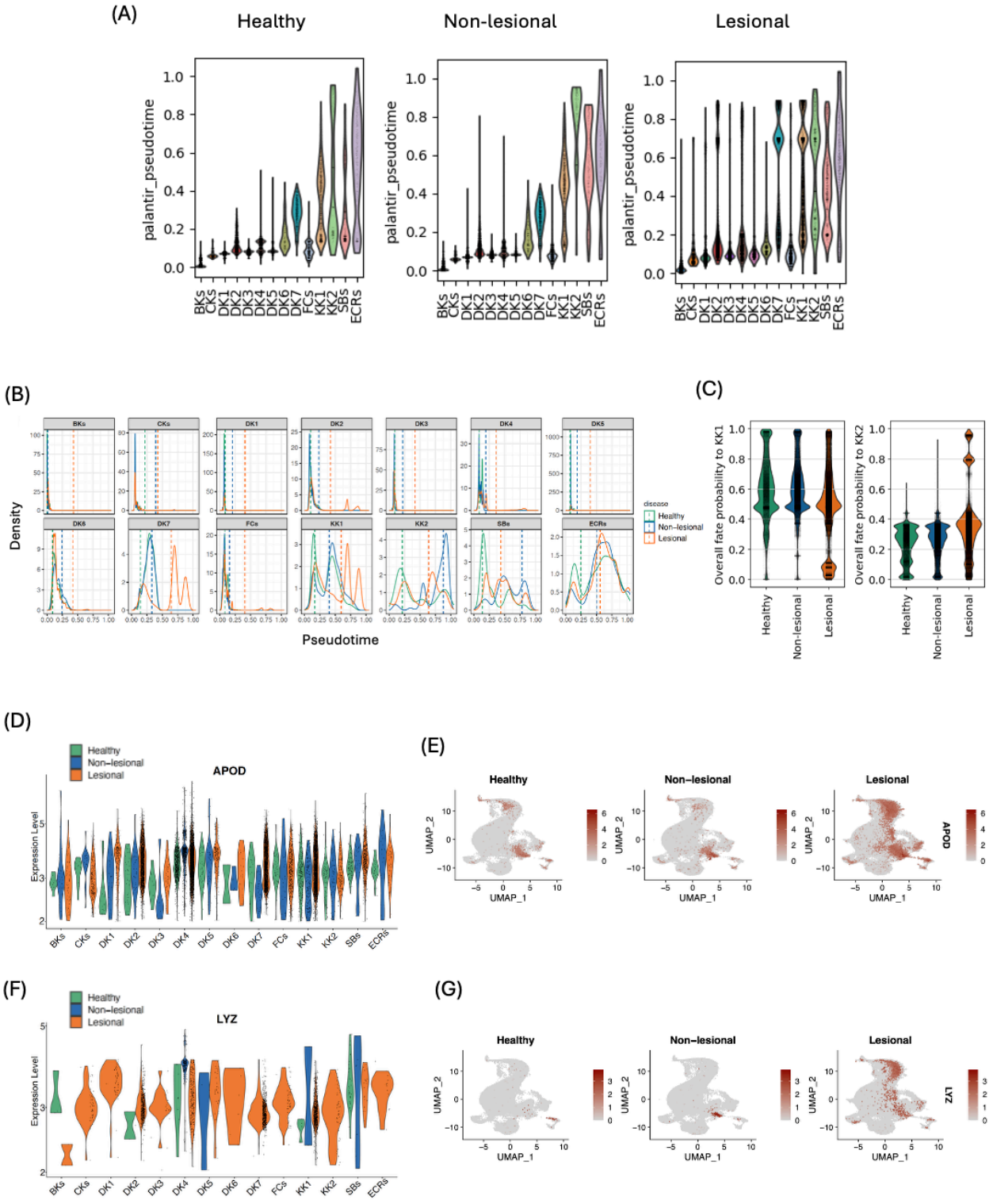

Supplementary Figure S5. Cell trajectory and transition probability in keratinocytes. (A) Violin plots showing the pseudotime distribution in individual keratinocyte subclusters, stratified by tissue types. (B) Pseudotime density plots within individual keratinocyte subclusters by tissue type. (C) Violin plots showing the cell fate probability of transitioning to KK1 or KK2 subclusters.

(D) Violin plots showing *APOD* expression in each subcluster, stratified by tissue types (only cells with *APOD* expression > 0 shown). (E) Feature plots of *APOD* expression in healthy, non-lesional and lesional AD samples. (F) Violin plots showing *LYZ* expression in each subcluster, stratified by tissue types (only cells with *LYZ* expression > 0 shown). (G) Feature plots of *LYZ* expression in healthy, non-lesional and lesional AD samples.

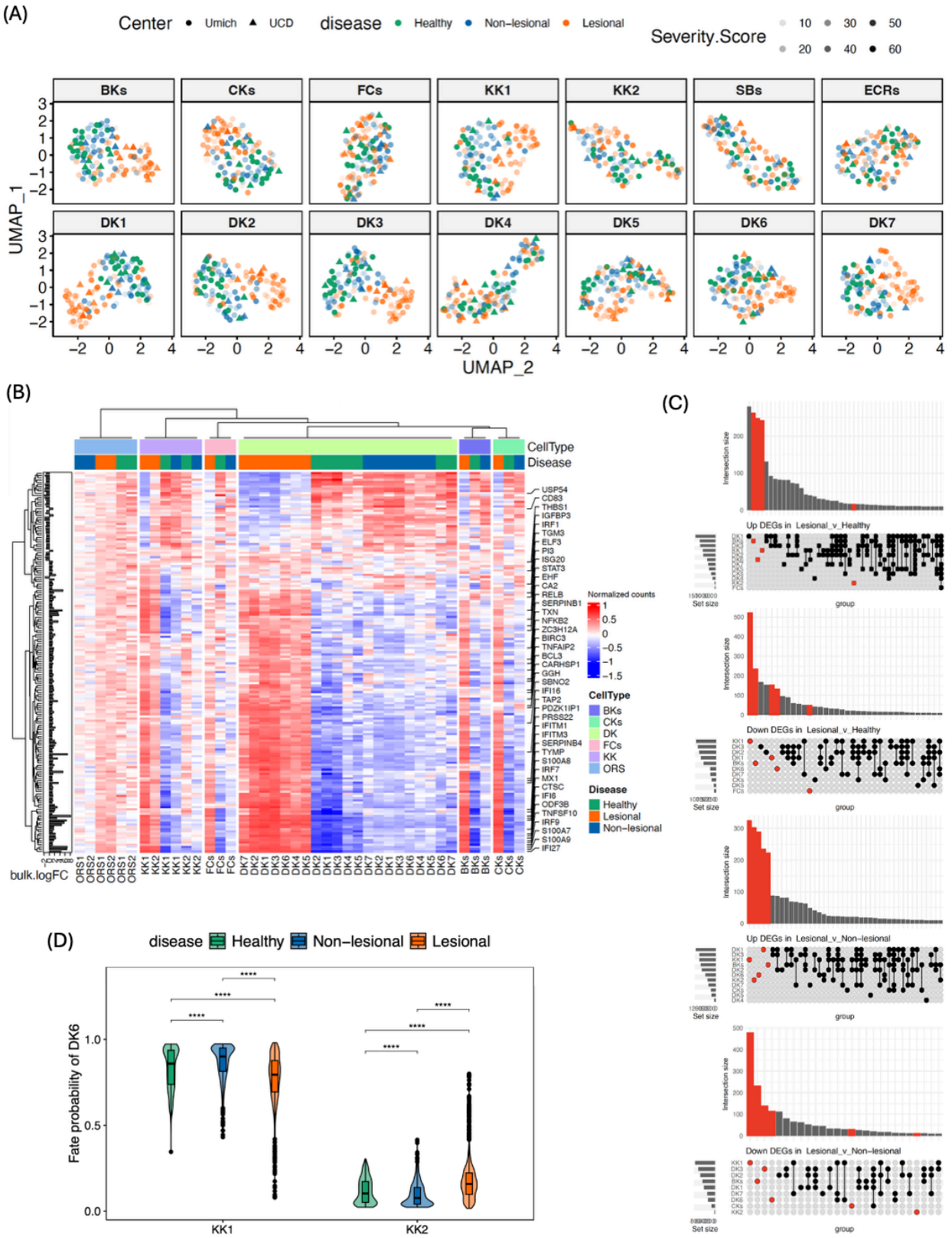
(A)
Center Umich UCD
disease Healthy Non−lesional Lesional
Severity.Score 10 20 30 40 50 60
BKs CKs FCs KK1 KK2 SBs ECRs
DK1 DK2 DK3 DK4 DK5 DK6 DK7
UMAP_1
UMAP_2
(B)
CellType
Disease
Normalized counts
CellType
BKs
CKs
DK
FCs
KK
ORS
Disease
Healthy
Lesional
Non−lesional
bulk.logFC
(C)
Up DEGs in Lesional_v_Healthy
Down DEGs in Lesional_v_Healthy
Up DEGs in Lesional_v_Non−lesional
Down DEGs in Lesional_v_Non−lesional
Intersection size
Set size
group
(D)
disease Healthy Non−lesional Lesional
Fate probability of DK6
KK1
KK2

Supplementary Figure S6. Pseudobulk analysis on keratinocytes subclusters. (A) UMAP visualization of sample clustering based on pseudobulk gene expression. (B) Heatmap showing the pseudobulk expression of differentially expressed genes (DEGs) identified from a previous bulk RNA-seq data comparing lesional AD (LAD) and healthy controls (HC). Cytokine responsive genes (i.e. the top-ranked bulk up-DEG genes for individual cytokine stimulations) are indicated. (C) UpSet plots showing the overlap of up- or down-DEGs across individual KC subclusters. The groups with greater than 20% non-overlap are highlighted in red. (D) Violin plots showing DK6 cell fate probabilities for transitioning towards KK1 or KK2 subclusters, stratified by tissue types (cell numbers: healthy, 425; non-lesional, 669; lesional, 2050). Two-sided Wilcoxon rank-sum test with BH-adjusted p values are shown (* p.adj < 0.05, ** p.adj < 0.01, *** p.adj < 0.001, **** p.adj < 0.0001).

(A)

Gene	stim	NTC	siRNA	FC
APOD	IL-13	0.0034	0.0028	0.8310
APOD	IL-22	0.0056	0.0019	0.3350
APOD	Untr	0.0054	0.0021	0.3930
LYZ	IL-13	0.0003	0.0002	0.5260
LYZ	IL-22	0.0007	0.0001	0.1320
LYZ	Untr	0.0002	0.0001	0.3030
SERPINB4	IL-13	0.2660	0.0851	0.3200
SERPINB4	IL-22	0.0091	0.0035	0.3860
SERPINB4	Untr	0.0080	0.0050	0.6240

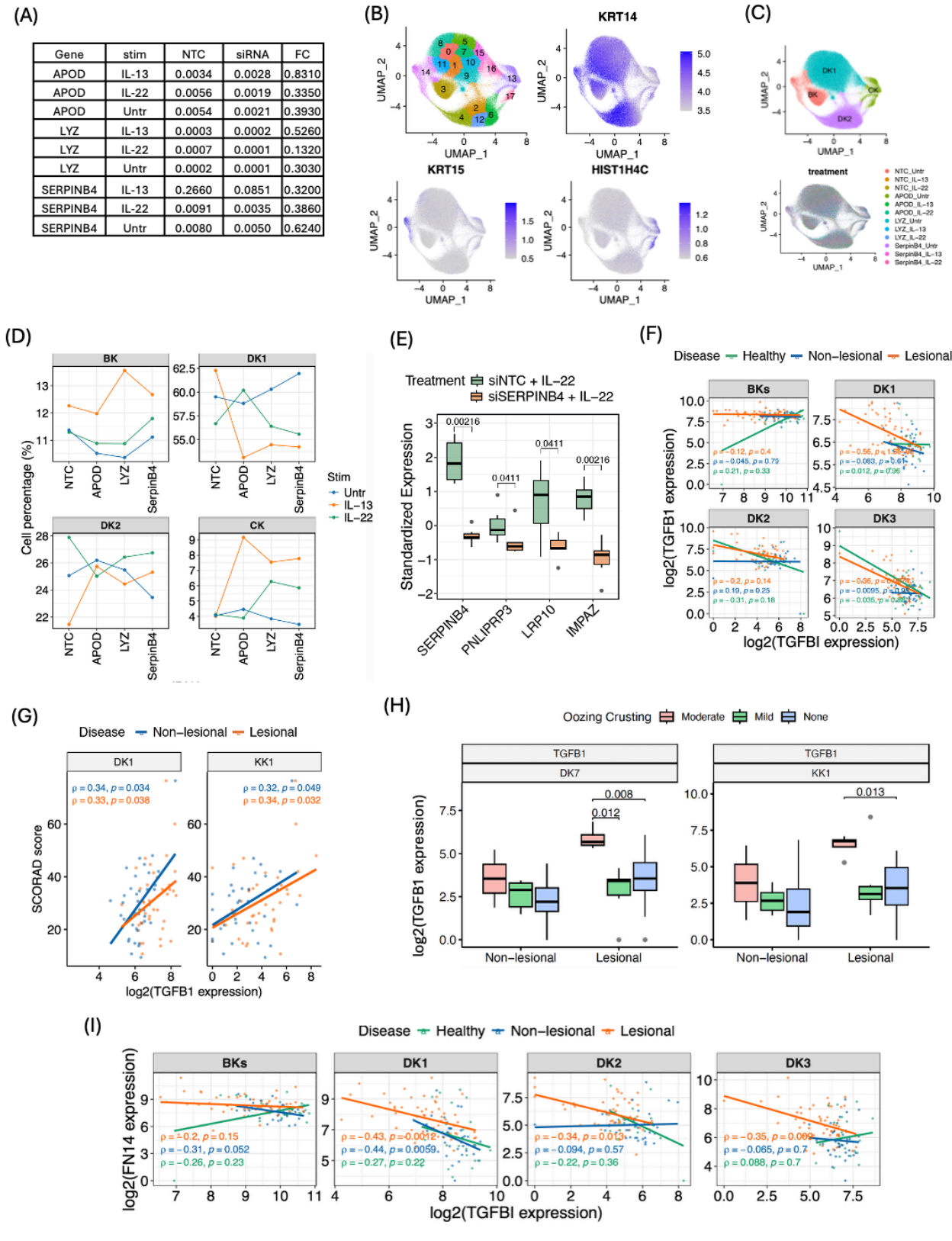

Supplementary Figure S7. scRNAseq analysis of *in vitro* cytokine-stimulated N/TERT cell line. (A) Average expression of the three siRNA-targeted genes in N/TERT cells under conditions with or without IL-13 or IL-22 stimulation, along with fold changes between siRNA-targeted and non-targeted (NTC) groups. (B) UMAPs colored by cell clusters and by expression of three marker genes (*KRT14*, *KRT15* and *HIST1H4C*). (C) UMAPs colored by cell types and by samples. (D) Cell proportions in individual cell types across siRNA conditions (NTC and siRNA targeting *APOD*, *LYZ* or *SERPINB4*). (E) Gene expression in 3D organotypic epidermal culturess treated with IL-22 and siRNA targeting either a non-targeting control (siNTC) or SERPINB4 (siSERPINB4). Standardized relative expression of four genes (*SERPINB4, PNLIPRP3, LRP10 and IMPA2*), assessed by qRT-PCR, is shown. A total of six samples were analyzed from two experiments, with three replicates per condition. (F) Correlation between *TGFBI* and *TGFB1* expression in BKs, DK1-3 subclusters specifically, stratified by tissue types. Spearman correlation coefficients and p values are indicated. (G) Correlation between *TGFB1* expression and SCORAD score in DK1 and KK1 subclusters. (H) Box plots showing *TGFB1* expression in non-lesional (N = 36) and lesional AD skins (N = 37) with moderate, mild or no oozing and crusting. (I) Correlation between *TGFBI* and *FN14* expression in BKs and DK1-3 subclusters, stratified by tissue types. E and H: Box plots display median (center line), interquartile range (box; 25th–75th percentiles), and whiskers extending to 1.5× IQR, with whisker limits defining the minimum and maximum values within this range. Two-tailed Wilcoxon rank-rum test p values < 0.05 are shown. F, G and I: Spearman rank correlation coefficients (ρ) and two-sided p values are shown.

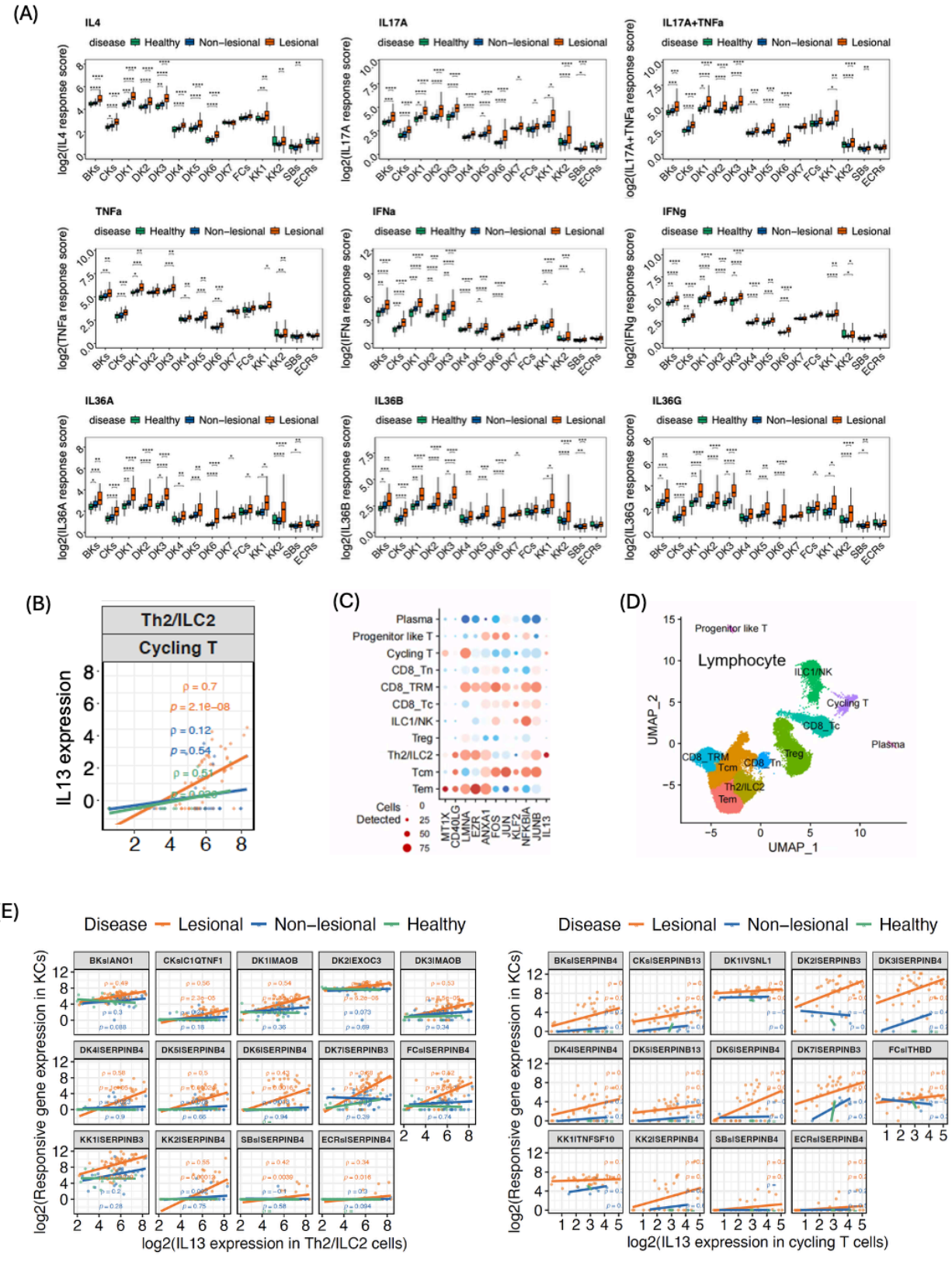
(A)
IL4
IL17A
IL17A+TNFa
TNFa
IFNa
IFNg
IL36A
IL36B
IL36G
disease Healthy Non−lesional Lesional
BKs CKs DK1 DK2 DK3 DK4 DK5 DK6 DK7 FCs KK1 KK2 SBs ECRs
(B)
Th2/ILC2
Cycling T
IL13 expression
ρ = 0.7
p = 2.1e−08
ρ = 0.12
p = 0.54
ρ = 0.51
p = 0.0039
(C)
Plasma
Progenitor like T
Cycling T
CD8_Tn
CD8_TRM
CD8_Tc
ILC1/NK
Treg
Th2/ILC2
Tcm
Tem
Cells Detected
0 25 50 75
MT1X CD40LG LMNA EZR ANXA1 FOS JUN KLF2 NFKBIA JUNB IL13
(D)
Progenitor like T
Lymphocyte
ILC1/NK
Cycling T
CD8_Tc
Plasma
CD8_TRM
Tcm
CD8_Tn
Treg
Th2/ILC2
Tem
UMAP_2
UMAP_1
(E)
Disease Lesional Non−lesional Healthy
BKsIANO1
CKsIC1QTNF1
DK1IMAOB
DK2IEXOC3
DK3IMAOB
DK4ISERPINB4
DK5ISERPINB4
DK6ISERPINB4
DK7ISERPINB3
FCsISERPINB4
KK1ISERPINB3
KK2ISERPINB4
SBsISERPINB4
ECRsISERPINB4
log2(Responsive gene expression in KCs)
log2(IL13 expression in Th2/ILC2 cells)
BKsISERPINB4
CKsISERPINB13
DK1IVSNL1
DK2ISERPINB3
DK3ISERPINB4
DK4ISERPINB4
DK5ISERPINB13
DK6ISERPINB4
DK7ISERPINB3
FCsITHBD
KK1ITNFSF10
KK2ISERPINB4
SBsISERPINB4
ECRsISERPINB4
log2(IL13 expression in cycling T cells)

Supplementary Figure S8. Cytokine response in keratinocyte subclusters. (A) Distribution of various cytokine responses across keratinocyte subclusters, stratified by tissue types. Box plots display median (center line), interquartile range (box; 25th–75th percentiles), and whiskers extending to 1.5× IQR, where whiskers define the minimum and maximum values within this range. Asterisks indicate the significance levels based on two-sided Wilcoxon rank-sum test with BH-adjusted p values (* p.adj < 0.05, ** p.adj < 0.01, *** p.adj < 0.001, **** p.adj < 0.0001). 23 healthy, 39 non-lesional and 54 lesional samples were included in the analysis. (B) Correlation of IL13 expression between Th2/ILC2 and cycling T cells, stratified by tissue types. (C) Average expression of marker genes for individual immune cell types. (D) UMAP showing lymphocyte sub-clustering. (E) Correlation between IL13 expression in Th2/ILC2 (left) or cycling T cells (right) with the top correlated gene's expression in the corresponding keratinocyte subclusters. B and E: Spearman rank correlation coefficients (ρ) and two-sided p values are shown.